



Strength assessment of Al-Humic and Al-Kaolin aggregates by intrusive and non-intrusive methods



Rodrigo B. Moruzzi^{a,d,*}, Pedro Grava da Silva^b, Soroosh Sharifi^c, Luiza C. Campos^d, John Gregory^d

^a Instituto de Geociências e Ciências Exatas, Univ. Estadual Paulista (UNESP), Av. 24-A, 1515, Jardim Bela Vista, Rio Claro, 13506-900 São Paulo, Brazil

^b Programa de Pós-graduação em Engenharia Civil e Ambiental, Univ. Estadual Paulista (UNESP), Av. 24-A, 1515, Jardim Bela Vista, Rio Claro, 13506-900 São Paulo, Brazil

^c Department of Civil Engineering, University of Birmingham, B15 2TT, United Kingdom

^d Department of Civil, Environmental and Geomatic Engineering, University College London, Gower St, London WC1E 6BT, United Kingdom

1

2

3

4 Rodrigo B. Moruzzi^{a*}, Pedro Grava da Silva^b, Soroosh Sharifi^c, Luiza C. Campos^d, John

5 Gregory^d

6

7 ^a Instituto de Geociências e Ciências Exatas, Univ. Estadual Paulista (UNESP), Av. 24-A,
8 1515, Jardim Bela Vista, Rio Claro, 13506-900. São Paulo, Brazil. E-mail:

9 rmoruzzi@rc.unesp.br

10 ^b Programa de Pós-graduação em Engenharia Civil e Ambiental, Univ. Estadual Paulista
11 (UNESP), Av. 24-A, 1515, Jardim Bela Vista, Rio Claro, 13506-900. São Paulo, Brazil. E-
12 mail: pedroagrava@gmail.com

13 ^c Department of Civil Engineering, University of Birmingham, B15 2TT, United Kingdom.
14 Email: S.Sharifi@bham.ac.uk

15 ^d Department of Civil, Environmental and Geomatic Engineering, University College London,
16 Gower St, London, WC1E 6BT, United Kingdom. E-mail: l.campos@ucl.ac.uk

17

18

19

20 **Address:**

21 * Corresponding author: Avenida 24-A, nº 1515, C. P. 178, CEP 13506-900, Office 23, Bela Vista,
22 Rio Claro, São Paulo, Brazil. Phone: +55 19 3526-9339. E-mail address: rmoruzzi@rc.unesp.br

23 **Abstract:**

24 Resistance to breakage is a critical property of aggregates generated in water and wastewater
25 treatment processes. After flocculation, aggregates should ideally keep their physical
26 characteristics (i.e. size and morphology), to result in the best performance possible by
27 individual separation processes. The integrity of aggregates after flocculation depends upon
28 their capacity to resist shear forces while transported through canals, passages, apertures,
29 orifices and other hydraulic units. In this study, the strength of Al-Humic and Al-Kaolin
30 aggregates was investigated using two macroscopic measurement techniques, based on both
31 intrusive and non-intrusive methods, using image analysis and light scattering based
32 equipment. Each technique generates different information which was used for obtaining
33 three floc strength indicators, namely, strength factor (SF), local stress from the
34 hydrodynamic disturbance (σ) and the force coefficient (γ) for two different study waters. The
35 results showed an increasing trend for the SF of both Al-Humic and Al-Kaolin aggregates,
36 ranging from 29.7% to 78.6% and from 33.3% to 85.2%, respectively, in response to the
37 increase of applied shear forces during flocculation (from 20 to 120 s^{-1}). This indicates that
38 aggregates formed at higher shear rates are more resistant to breakage than those formed at
39 lower rates. In these conditions, σ values were observed to range from 0.07 to 0.44 N/m^2 and
40 from 0.08 to 0.47 N/m^2 for Al-Humic and Al-Kaolin, respectively. Additionally, it was found
41 that for all studied conditions, the resistance of aggregates to shear forces was nearly the same
42 for Al-Humic and Al-Kaolin aggregates, formed from destabilized particles using sweep
43 coagulation. These results suggest that aggregate strength may be mainly controlled by the
44 coagulant, emphasizing the importance of the coagulant selection in water treatment. In
45 addition, the use of both intrusive and non-intrusive techniques helped to confirm and expand
46 previous experiments recently reported in literature.

47

48 **Keywords:** Aggregates, floc resistance, image analysis, flocculation.

1. Introduction

Most solid-liquid separation processes work by increasing the size of the particulate matter, leading to the formation of aggregates or flocs. The performance of solids removal is dependent on the physical characteristics of the aggregates that need to be compatible with the separation method used (Yukselen and Gregory, 2004). Among these characteristics, the floc strength, which is an expression of resistance to breakage, is crucial for effective particle separation in clarification units, such as sedimentation tanks, dissolved air flotation units and membrane filtration (Jarvis *et al.*, 2005).

It is well-documented that, solid-liquid processes are negatively affected by the breakage of flocs, as only limited regrowth of broken flocs can occur, thus leading to low removal efficiency in sedimentation units (Yukselen and Gregory, 2002, 2004; Yu *et al.*, 2010b, 2011, 2015). The floc strength is also linked to problems in treatment plants with rapid sand filtration, in which the small resistance of the aggregates to the hydrodynamic variations has a damaging impact on the filter media, shortening their operational life and resulting in pollutant trespassing (Moruzzi and Silva, 2018). Therefore, water treatment plants should ideally be designed to minimize floc breakage; however, despite the recommendations, it is difficult to precisely determine how much stress a previously formed floc can take without breaking.

When the shear rate is larger than floc strength, the flocs either break into approximately equal size fragments, or under some circumstances, erosion of small particles from the flocs' surface may occur. In turbulent flow, the breakage type depends on the size of the flocs in relation to the micro-scale of turbulence (Mühle, 1993). Because of floc breakage, some regions of the floc surface may become inactive and incapable of forming new bonds of attachment to other flocs, thus reducing the flocculation efficiency (Yu *et al.*, 2011). The fact that broken flocs do not fully regrow when the original low shear rate is restored means that the binding between particles is weaker (Yu *et al.*, 2010b).

It is well acknowledged that the floc strength is dependent on the bonds between aggregate component particles (Parker *et al.*, 1972, Bache *et al.*, 1997). This includes the strength and number of individual bonds within the floc. However, recent studies (e.g. Yu *et al.*, 2015) have shown that kaolin particles incorporated within hydroxide flocs appear to have no influence on floc properties, including floc strength and size. Younker and Walsh (2016) demonstrated that the addition of adsorbents to metallic salt flocs did not increase or reduce

81 flocculation strength. Conversely, kaolin flocs formed by ferric coagulants were found to be larger
82 and stronger than those formed by alum coagulants (Zhong *et al.*, 2011). Bridging
83 flocculation by long-chain polymers can generate very resistant flocs, while the
84 destabilization of particles by low dosages of inorganic salts results in fairly weak flocs
85 (Yukselen and Gregory, 2004; Wang *et al.*, 2009; Yu *et al.*, 2015).

86 Humic acids have been widely used as natural organic matter to investigate floc properties
87 after flocculation. It has been shown that humic flocs growth is not determined by the flocs'
88 size distribution (Yu *et al.*, 2010b, 2012), but by some of their properties, including floc
89 strength, which is mostly dependent on the surface activity of flocs, and coagulant species
90 formed from Alum and Iron hydrolysis (Wang *et al.*, 2009).

91 Moruzzi and Silva (2018) carried out experiments on Al-Humic and Al-Kaolin aggregates and
92 showed that flocs formed from sweep coagulation mechanism, by different particulate matter
93 and the same coagulant have similar regrowth patterns, indicating similar binding between
94 particles for Al-Humic and Al-Kaolin, as presented by Yu *et al.* (2010b). On the basis of these
95 findings, it is speculated that Al-Humic flocs strength might have similar resistance to shear
96 forces as Al-Kaolin flocs. In this case, the resistance of the flocs to shear rate could be
97 attributed to the used coagulant, corroborating with results presented by Yu *et al.* (2015).

98 For determining aggregate properties, such as size and floc strength, monitoring techniques
99 should be applied during flocculation. Intrusive techniques, such as those based on light
100 scattering, have been conventionally used for monitoring aggregates during flocculation
101 (Yukselen and Gregory, 2002; 2004; Yu *et al.*, 2011). However, these techniques require
102 taking frequent samples from the water into measurements chambers, a process that may
103 cause some damage to aggregates due to their fragile nature. In some cases, flocs damage may
104 be minimized by limiting the average gradient velocity during the sample extraction,
105 controlling inner tube size and flow through tube, as presented by Gregory (1981) and Yu *et al.*
106 (2010b). Recently, however, flocculation monitoring by non-intrusive image analysis has
107 shown promising results (Li *et al.*, 2007; Moruzzi *et al.*, 2017; Moruzzi and Silva, 2018) and
108 has allowed the determination of floc strength, among other floc characteristics.

109 In practice, the strength of the floc is often determined in an empirical way, usually by
110 establishing a relationship between the floc size and the applied shear rate (François, 1987;
111 Jarvis *et al.*, 2005, Li *et al.*, 2007). This empirical approach was firstly suggested by Parker *et*

112 *al.* (1972), and it has been used extensively in theoretical and experimental research to
113 evaluate maximum floc size under a given turbulent intensity (e.g. Bache, 1989; 2004 and Li
114 *et al.*, 2006; 2007).

115 There are two fundamental approaches to measuring the strength of the floc *i.e.* a macroscopic
116 approach, which measures the system energy required for breakage of flocs, and a
117 microscopic approach, which measures the interparticle forces within individual flocs (Jarvis
118 *et al.*, 2005). In the microscopic approach, the strength can be measured by applying a shear
119 stress or a normal stress to a floc individually. On the other hand, macroscopic techniques
120 perform an indirect evaluation of the floc resistance by means of analysing the energy
121 dissipation, or the mean velocity gradient (G), applied to maximum- or average-sized flocs.
122 This approach originated from the empirical relationship between the applied hydrodynamic
123 shear rate and the resulted floc size (Jarvis *et al.*, 2005).

124 This work aims to investigate the floc strength for both Al-Kaolin and Al-Humic aggregates
125 by means of macroscopic indicators, and to demonstrate the insignificant effect of the
126 particulate matter within the flocs on their properties, namely size and strength. For the first
127 time, image analysis is applied concomitantly with photometric dispersion to obtain the
128 strength factor (SF), local stress from the hydrodynamic disturbance (σ) and the force
129 coefficient (γ). The combined application permits the comparison and establishment of
130 correlations between the data obtained from two different techniques (intrusive and non-
131 intrusive). This is the first time image and photometric dispersion of Al-Humic acid flocs is
132 measured by this technique and the results from the two complementary methods is used to
133 understand the factors affecting floc strength.

134 **2. Materials and Methods**

135 *2.1 Study Waters*

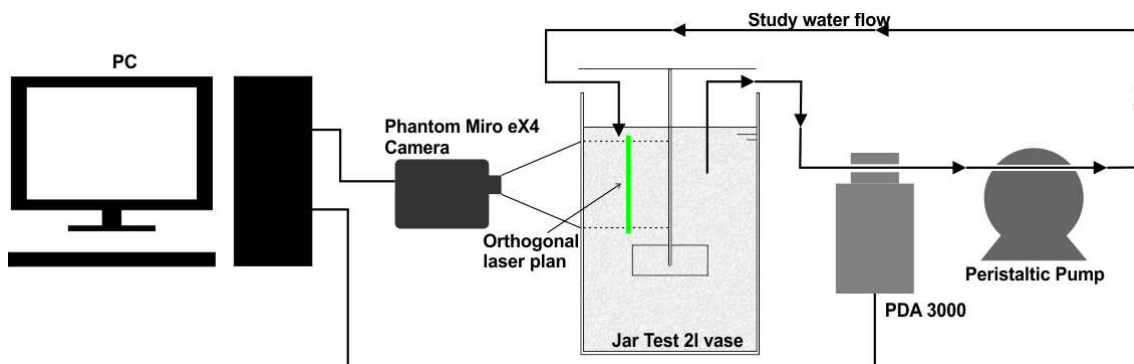
136 Two water samples were prepared from stock suspension of kaolin and from stock solution of
137 humic acid. For sample one, hereafter referred to as type 1, a humic acid solution prepared
138 from lyophilised natural organic matter (*Aldrich Chemical*) with concentration of 30 mg/L
139 was used to obtain 50 units of Platinum-Cobalt Scale - PtCo at 455 nm, as the initial
140 condition (Moruzzi and Silva, 2018). For the second sample (type 2), a kaolin suspension was
141 prepared from a commercial kaolin (Sigma-Aldrich) to obtain 25 units of turbidity scale as
142 Nephelometric Turbidity Units - NTU (Moruzzi *et. al.*, 2017 and Yukselen and Gregory,
143 2004).

144 Coagulation was performed by dosing alum $[\text{Al}_2(\text{SO}_4)_3 \cdot 18\text{H}_2\text{O}]$ using sweep-coagulation
145 mechanism, following recommendations by Oliveira *et al.* (2015). So, dosages of 10 and 30
146 $\text{mgAl}^{+3}/\text{l}$ at pH of 7.5 and 4.5 were applied for Al-Kaolin and Al-Humic aggregates
147 formation, respectively. Sodium hydroxide (NaOH) 1 mM was used as a buffer during
148 coagulation to control pH. All tests were performed at room temperature ($20 \pm 2^\circ\text{C}$).

149 2.2 Flocculation and strength tests

150 Jar tests were performed for flocculation and breakage experiments (*Ethik Technology Model*
151 *218/6 LDB*). The method applied consists of an intrusive and non-intrusive image-based
152 acquisition method and photometric dispersion analyser (PDA), similar to that used by Yu *et*
153 *al.* (2015). Here, however, both image and photometric dispersion were applied at the same
154 time to obtain strength indices, thus permitting comparison and correlation of results. A
155 simplified schematic of the experimental apparatus, including Jar Test, the image-based
156 system and light-scattering monitoring equipment, is shown in Figure 1.

157 A mean velocity gradient of 800 s^{-1} was applied for 10 seconds to ensure a rapid mixing, and
158 also for flocs breakage in all light scattering tests, based on preliminary tests (Oliveira *et al.*,
159 2015). This standard shear rate was chosen for taking a central position in the typical shear
160 range of predominant erosion breakage as proposed by Mikkelsen and Keiding (2002), and
161 the duration was sufficient for the coagulant transportation (Yukselen and Gregory, 2004).
162 For flocculation, the following velocity gradients (G) were applied: 20, 30, 40, 50, 60, 80, 100
163 and 120 s^{-1} . For the trials involving PDA measurements, G values were kept constant during
164 the first 25 minutes, and after this period, G was set to 800 s^{-1} for 10 seconds to induce
165 breakage of flocs. This short period of time was chosen to simulate the water passage in gates
166 and orifices that normally occur after flocculation.



167
168 Figure 1. A simplified schematic of the experimental apparatus.
169

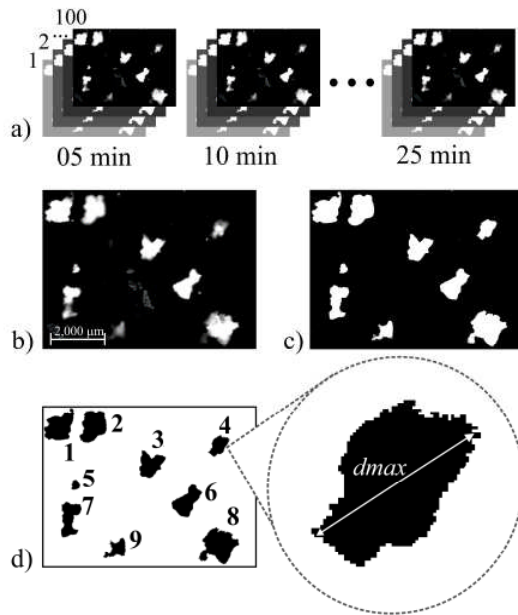
170 2.3 Image Analysis

171 The image analysis applied here was strictly used to obtain aggregates size, which in turn was
172 used for floc strength indicator calculations, namely local stress from the hydrodynamic
173 disturbance (σ) and the force coefficient (γ), as presented in Section 2.6. Images were
174 captured in 2^8 bit monochromatic mode (*i.e.* 256 grey scale) using a *Vision Research Miro*
175 *EX4* camera together with a set of lenses, and 840 pixel x 640 pixel of image resolution, to
176 obtain a pixel size of 10 μm . A laser sheet of 20,000 mW and wavelength of 520 nm provided
177 the lighting as described by Oliveira *et al.* (2015) and Moruzzi *et al.* (2017).

178 Samples were obtained at 5-minute intervals (from 5 to 25 minutes) to assess floc size at a
179 given flocculation time (T) of interest, *i.e.* those usually applied in drinking water treatment
180 plants. Each image package was taken over a short duration of 10 seconds with a frequency of
181 10 Hz (Figure 2-a) to precisely describe the system situation at that given time of interest.
182 This sample time and frequency was sufficient to capture a reliable picture of the floc
183 characteristics at the required flocculation time along with a statically representative number
184 of flocs within the 10 seconds sampling time.

185 The image processing software *Image-Pro-Plus*® (IPP) was used to develop the images, *i.e.*
186 conversion from 2^8 to 2^1 bits, enhancement and measurement (Figures 2-b to 2-d). Only
187 aggregate sizes longer than 100 μm (≥ 10 pixels) were monitored for image precision, as
188 recommended by Chakraborti *et al.* (2003).

189 In total, 197,207 aggregates were measured from 7,200 frames (average of 27
190 aggregates/frame) for Al-Humic water, and 141,609 aggregates were measured from 6,800
191 frames (average of 21 aggregates/frame) for Al-Kaolin water. In these sample sizes, floc size
192 errors were lower than 4.0% and 4.6% at 95% of confidence interval for an infinite population
193 of Al-Humic and Al-Kaolin aggregates, respectively. Figure 2 illustrates the different steps
194 involved in the image processing procedure applied here, from acquisition to image
195 processing and size measurement.



196

197 Figure 2. An example of image conversion enhancement and measurement: (a) Image
 198 acquisition using on 10 Hz during 10 seconds for each flocculation time (T), resulting in a
 199 pack of 100 frames per $G \times T$; (b) Flocs in grey scale (2^8 bits); (c) Image after threshold
 200 with black and white pixels only (2^1 bits); (d) Counting and measuring flocs by IPP 7.0 software®.

201 2.4 Light Scattering

202 The light scattering approach applied was strictly used to obtain the flocculation index (FI),
 203 which will be better explained in the following sections. Light scattering analysis was
 204 performed using a *Photometric Dispersion Analyser* (PDA), and the obtained results were
 205 used for calculating the strength factor, which will be introduced and presented in Section 2.6.
 206 In PDA equipment, samples flow through a 3-mm-diameter tube where the intensity of a
 207 narrow beam of light is monitored by a sensitive photodetector following Yukselen and
 208 Gregory (2004) and Moruzzi *et al.* (2017). Although intrusive technologies can cause some
 209 damage to flocs, in PDA this can be minimised by controlling the average gradient velocity
 210 during sample extraction. Here, the flow rate through the sampling tube was controlled to
 211 enforce laminar flow regime (Reynolds number ≤ 80) and shear rates lower than 50 s^{-1} , as
 212 shown by Gregory (1981); conditions where damage is considered insignificant, as also
 213 shown by Yu *et al.*, 2010b. Further, the water samples were circulated by means of a
 214 peristaltic pump located after the PDA instrument to avoid the effects of possible floc
 215 breakage in the pinch part of the pump (Figure 1), as performed by Li *et al.* (2007).

216 The *PDA 3000* measures the average transmitted light intensity (dc value) and the root mean
217 square (rms) value of the fluctuating component. The ratio (rms/dc) provides a measure of the
218 balance of particle aggregation (Gregory, 1984; Gregory and Nelson, 1986; Yukselen and
219 Gregory, 2004; Yu *et al.*, 2010b), hereafter referred to as flocculation index (*FI*). Up to a
220 limited size, the *FI* value is strongly correlated with floc size and always increases as flocs
221 grow larger, but the *FI* value can become uncertain when flocs are larger than 250 μm and
222 absolute floc size cannot be taken from *FI* signals (Yu *et al.*, 2010a; Yu *et al.*, 2010b and
223 2011). Also, larger aggregates have a predominant influence on the ratio value (Gregory,
224 1984), thus affecting *FI* signals. Therefore, the PDA shows qualitative changes in flocs, as
225 reported by Gregory and Nelson (1986), but the instrument is unable to give an absolute
226 particle size. Further, the *FI* signals vary with both particle size and particle number and it is
227 not possible to know the precise contribution of each of these components in the *FI* signal. Yu
228 *et al.* (2015) have shown that flocs with similar size can have very different *FI* values,
229 confirming the idea that *FI* does not give an absolute indication of size for hydroxide flocs.
230 However, the generated signal can be used as an indicator of aggregation, as shown by
231 Gregory (1985), and also as a measure of floc strength as shown by Li *et al.* (2007), Gregory
232 (2009) and Yu *et al.* (2010b). More details are given in the following sections.

233

234 2.5 Floc size and *FI* determination

235 The macroscopic techniques used for the study of the floc strength were developed based on
236 the relationship between the applied hydrodynamic shear rate and the resulting floc size.
237 According to Gregory (2003), floc size and *FI* can be both used as floc strength indicators for
238 a given shear rate. In order to obtain the floc strength indicators, which are related directly to
239 the size limit reached by the floc, two different sources of information were utilized: one from
240 the image analysis and another from the PDA.

241 For image analysis, the average diameter (d) of aggregates was determined from the average
242 of the longest length of the aggregates (d_{max}) in the selected times of interest, following Li *et*
243 *al.* (2007):

244

$$245 \quad d = \frac{1}{n} \sum_{i=1}^n d_{imax} \quad (1)$$

246 where d is the average of d_{max} (μm), d_{max} is the longest length (μm), as shown in Figure 2, and
247 n is the number of counted aggregates in a sample varying from $i = 1, 2 \dots, n$.

248 The d values obtained from Equation 1 represents the average of d_{max} , measured for each one
249 of the eight investigated flocculation times (T), *i.e.* 5, 10, 15, 20, 25, 30, 35 or 40 minutes. It
250 is important to emphasize that, flocculation kinetics were not the focus of this paper, but
251 rather the floc strength assessment at given flocculation times of interest, where the dynamic
252 equilibrium between flocs breakage and aggregation could be indirectly observed by the floc
253 size. Therefore, the d value represents the balance between flocs aggregation and breakage at
254 a given time of flocculation, and its average size tends to a stable value, *i.e.* a limiting size, for
255 a given shear rate as the steady state regime is reached. When little variation is observed in
256 floc size, the average size of d remains oscillating slightly around a maximum value, which is
257 referred to as the plateau.

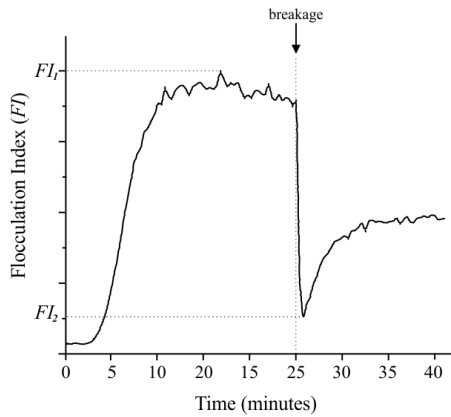
258 The plateau was determined from the incremental variation of the average diameter (d) during
259 flocculation. This variation tends to a narrow range because of the dynamic steady state. The
260 incremental variation can be determined by:

$$261 \quad \Delta d_i = \left| \frac{(d_i - d_{i-1})}{d_i} \right| \quad (2)$$

262 where Δd_i is the incremental variation of average diameter between the time interval $t_i - t_{i-1}$,
263 with $i = 1, 2, \dots, n$.

264 The typical value of the diameter in the plateau was then determined from the average of
265 diameters within $\Delta d \leq 10\%$. Hypothesis tests were also performed to confirm the plateau with
266 significance of 0.05.

267 The analysis based on light scattering was done through the FI signal generated from the
268 PDA. The maximum value observed in the stationary flocculation phase was adopted once the
269 plateau was reached at that time interval. For FI_2 , the value adopted was the minimum point at
270 the instant of the induced rupture, following Li *et al.* (2007). Here, the rupture shear rate of
271 800 s^{-1} was applied for 10 seconds, at the flocculation time of 25 minutes. Figure 3
272 schematically shows how FI_1 and FI_2 are determined from the FI signal.



273

274 Figure 3. Schematic representation of the FI signal, with indication of the values of FI_1 , FI_2
 275 and induced breakage by applying velocity gradient of 800 s^{-1} at 25 minutes (adapted from Li
 276 *et al.*, 2007).

277

278 2.6 Floc strength indicators

279 As mentioned in previous sections, the floc strength indicators presented here were
 280 determined using both image analysis and PDA. For the image analysis method, d values
 281 were taken, whilst for PDA only FI signals were used.

282 Floc strength coefficient (γ)

283 The floc strength coefficient (γ) was obtained from image analysis using Equation 3 that
 284 describes the stable size determined from image analysis as a function of the mean velocity
 285 gradient applied to the system during flocculation, firstly suggested by Parker *et al.* (1972):

$$286 \quad d = C \cdot G^{-\gamma} \quad (3)$$

287 where C is the multiplicative constant ($\mu\text{m/s}$), G is the average velocity gradient (s^{-1}), and γ
 288 is the floc strength coefficient (dimensionless), obtained from stable floc size.

289 The floc strength coefficient (γ) can be calculated using mean, median and longest length of
 290 flocs with nearly the same results, as reported by Leentvaar and Rebhun (1983). For the
 291 results presented here, d values were calculated using the longest length of flocs obtained
 292 during flocculation from different shear rates according to Equation 1.

293 The $\ln-\ln$ plot of Equation 3 against the average gradient velocity applied during flocculation
 294 results in a line, which its slope is indicative of floc strength. The inverse relationship of
 295 proportionality indicates that the higher the value of γ , the more prone the floc is to breakage
 296 under increasing shear rates, resulting in smaller aggregates (Li *et al.*, 2007). Therefore, the

297 value of γ is considered as an indicator of its strength. This concept was proposed by Parker *et*
298 *al.* (1972) and is adopted in the study of Li *et al.* (2007). Here, the floc strength coefficient (γ)
299 was determined from the slope of linear best fit to the *ln-ln* plot of Equation 3, using
300 experimental data for the study waters. It is worth noting that the value of C can also be used
301 as a floc strength indicator, but only within the same experimental conditions, as its value
302 depends upon the method used for particle size measurements and the choice of the
303 characteristic value of d (Jarvis *et al.*, 2005).

304 *Strength factor (SF)*

305 The strength factor (SF) has been previously used by several researchers (*e.g.* Li *et al.*, 2007;
306 Yu *et al.*, 2010b and 2015; Su *et al.*, 2017) to compare the breakage and the strength of flocs
307 in different shear rate conditions for Al-Kaolin aggregates. The results of these studies
308 indicate that this parameter can be effectively used as a floc strength index. SF is calculated
309 based on FI signals only and used to characterize the aggregate size maintenance capacity,
310 following Yukselen and Gregory (2002):

$$311 \quad SF (\%) = \frac{FI_2}{FI_1} 100 \quad (4)$$

312 where FI_1 is the maximum FI value before breakage, and FI_2 is the FI value right after the
313 breakage period, as shown in Figure 3. In this study, FI_1 was calculated from different shear
314 rates and FI_2 was always determined after applying a shear rate of 800 s^{-1} , as described in
315 Section 2.5.

316 High values of the SF indicate that flocs are better able to withstand shear rates, and therefore,
317 the higher the value of SF , the stronger the flocs can be considered for a given rupture shear
318 rate (Jarvis *et al.*, 2005). It is important to note that SF is not constant, the shear rate applied
319 during the breakage strongly affects FI_2 (Yu *et al.*, 2010b), and so, SF can only be compared for
320 similar induced rupture conditions. Here, the average velocity gradient of 800 s^{-1} was applied
321 for rupture.

322 *Hydrodynamic disturbance (σ)*

323 In addition to the above-mentioned empirical methods for obtaining a force coefficient, Bache
324 *et al.* (1997) proposed a theoretical method where the mean force applied per unit area of the
325 system, σ (N/m^2), could be determined by:

326
$$\sigma = \frac{4\sqrt{3}}{3} \frac{\rho_w \mathcal{E}^{3/4} d}{\nu^{1/4}} \quad (5)$$

327 where ρ_w is the density of the water (kg/m³), \mathcal{E} is the local energy dissipation rate per unit
 328 mass (m²/s³), d is the average of the longest length of aggregates at a given time, measured by
 329 image analysis (m) and ν is the kinematic viscosity (m²/s) at room temperature of $20 \pm 2^\circ\text{C}$.
 330 Parameter \mathcal{E} is usually replaced by $\overline{\mathcal{E}}$ (Equation 6), which is the average rate of dissipation of
 331 the local energy per unit mass and is directly proportional to G , a parameter easily
 332 administered during the experiment:

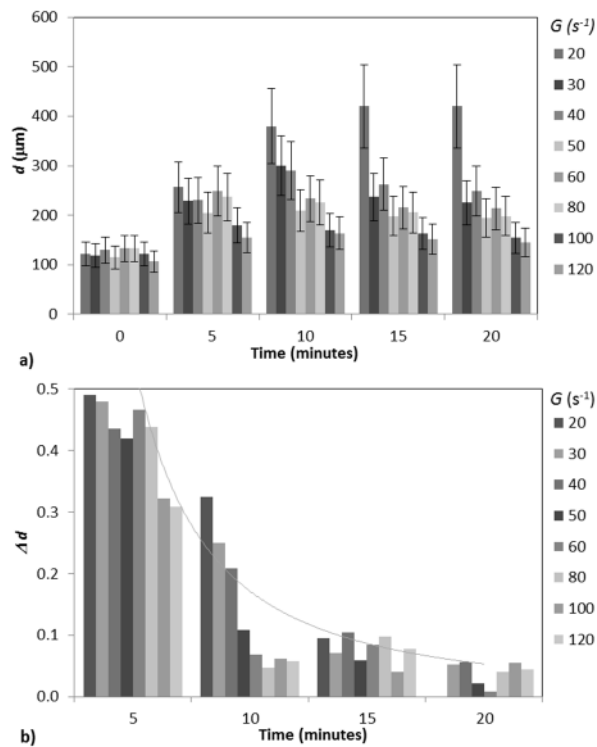
333
$$\overline{\mathcal{E}} = \nu G^2 \quad (6)$$

334 where ν is the kinematic viscosity (m²/s).

335 **3. Results and Discussion**

336 *3.1 Image analysis*

337 Figure 4, as an example, presents the time evolution of d and Δd obtained from Equations 1
 338 and 2, respectively, for various velocity gradients (G) applied to study water type 2. For d
 339 evolution (Figure 4-a), aggregates have grown for time intervals between 5 and 10 minutes
 340 and for G from 20 to 40 s⁻¹. After 10 minutes of flocculation, only G of 20 s⁻¹ has resulted in
 341 aggregates increment for d . Consequently, the incremental variation of floc size (Figure 4-b)
 342 is observed to be smaller than 10% for the majority of the analysed velocity gradients during
 343 the flocculation at times 10-15 and 15- 20 minutes (except for G of 20, 30 and 40 s⁻¹),
 344 indicating the establishment of steady-state conditions. Thus, d was obtained by averaging d
 345 during the period 15-20 minutes, when significant stability was observed, *i.e.* when the stable
 346 size of d was reached. For these time intervals, test of hypothesis has shown that there is no
 347 significant difference between the two water types for p-value of 0.05, *i.e.* for both Al-Humic
 348 and Al-Kaolin the average diameter did not change for time intervals from 15 to 20 minutes,
 349 making it possible to confirm the plateau.



350

351

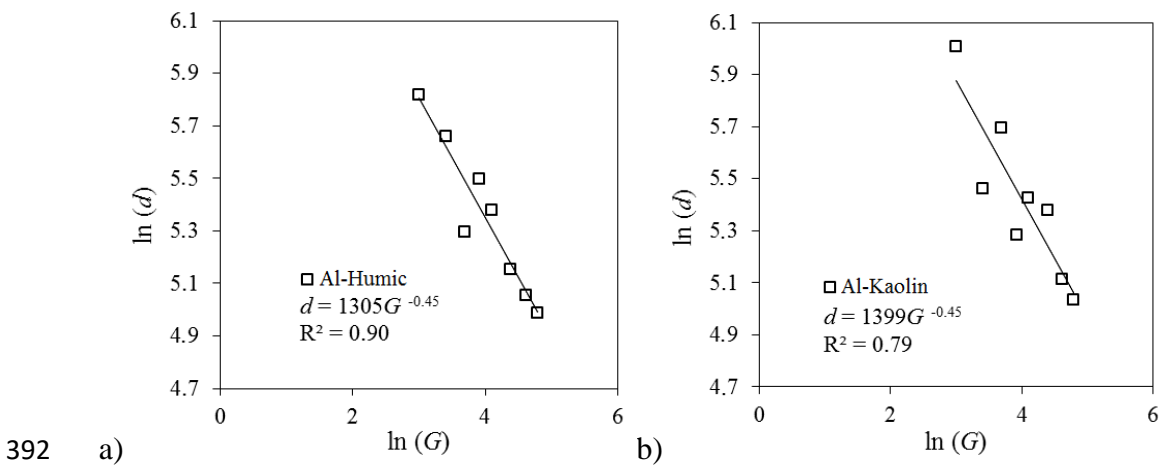
352 Figure 4. Time evolution of (a) d and (b) Δd during flocculation time (for discrete intervals of
 353 5, 10, 15 and 20 minutes) for water type 2. Fluctuation bars in (a), represent standard
 354 derivations and the decay curve in (b), represents the overall trend of Δd during time. Time
 355 zero in Fig. 4-a shows flocs size measurements in the very beginning of flocculation and those
 356 results were used as d_{i-1} for Δd calculation in time of 5 minutes, as Equation 2.

357 Figure 5 shows the relationship between $\ln(d)$, calculated by Equation 1, and $\ln(G)$, where
 358 the slope of the trend line, as described by Equation 3, indicates the floc strength coefficient γ ,
 359 Once γ value remains constant, any variant characteristic of d (*i.e.* mean, median or maximum
 360 length) can be used for comparing results among different studies (Jarvis *et al.*, 2005). A
 361 decreasing tendency of the stable size d in response to the increase of G was observed at a rate
 362 near 0.45 for the two study waters, which is in the range of 0.44 to 0.63 reported by other
 363 researchers (*e.g.* Bache and Rasool, 2001; Francois, 1987; Li *et al.*, 2007) when using alum as
 364 coagulant for Al-Humic and Al-Kaolin flocs.

365 The obtained γ value for the two study waters indicates that Al-Humic and Al-Kaolin flocs are
 366 similarly able to resist shear rates, as the steepness of the \ln - \ln plot slopes are nearly the same
 367 for both waters (0.45). The analysis of C from Equation 3 is not commonly used for floc
 368 strength evaluation, as it depends upon which characteristic of d has been used, and wide
 369 variation between different studies has been reported, *e.g.* from $\ln C$ of 7.1 to 9.4 according to

370 Bache *et al.* (1999) and Bache and Rasool (2001), respectively. However, C can be also used
 371 to compare floc strength within specific experimental system (Jarvis *et al.*, 2005). Results
 372 presented here have shown C values of 1305 ($\ln C$ of 7.17) and of 1399 ($\ln C$ of 7.24) for Al-
 373 Humic and Al-Kaolin, respectively, thus reinforcing that Al-Humic and Al-Kaolin have
 374 nearly the same ability to resist applied shear forces. These results are in agreement with the
 375 finding by Yu *et al.* (2015) who found that the nature of primary particles has no influence on
 376 floc strength when sweep coagulation mechanism is applied and once flocs rapidly grow and
 377 incorporate most particles within the hydroxide precipitate. Also, the use of a non-intrusive
 378 technique, such as the image analysis system here applied, permits to confirm the previous
 379 findings by Yu *et al.* (2015), once it is not influenced by possible interferences caused by
 380 samples extraction and light scattering, as presented by Gregory (2009) and Yu *et al.* (2015).

381 The analysis of strength coefficient (γ) can also be related to turbulent shear patterns due to
 382 eddy size, as proposed by Biggs and Lant (2000) and Bache (2004), resulting in different floc
 383 breakage modes during flocculation. Based on the analysis of the dominant mode of floc
 384 degradation presented by Parker (1972) and François (1987), the results presented here for γ
 385 (Figure 5) indicate that the flocs are more prone to breakage due to a dominant effect of
 386 fragmentation, as the result of the viscous energy dissipation, once the floc strength
 387 coefficient γ was around the theoretical value of 0.5. This is an indication that small eddies
 388 (*i.e.* the turbulence micro-scale) is of a similar order of magnitude to the flocs sizes (Mühle,
 389 1993; Jarvis *et al.*, 2005). However, fragmentation and erosion are expected to occur at the
 390 same time, as large flocs in an aggregated system may be larger than the micro-scale whilst
 391 smaller flocs may be smaller than micro-scale (Biggs and Lant, 2000).

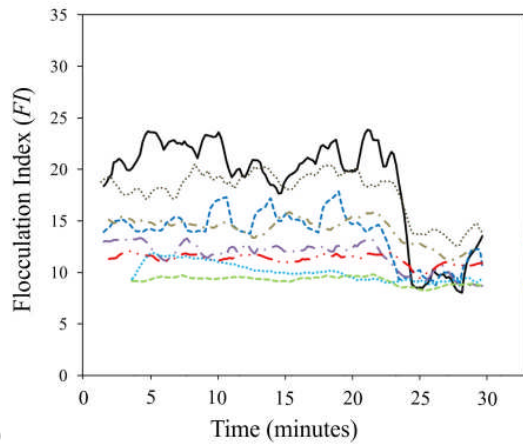


393 Figure 5. Relationship between $\ln d$ versus $\ln G$ during flocculation: (a) water type 1 – Al-
394 Humic and (b) water type 2 – Al-Kaolin. $\ln d$ was obtained by averaging d during the period
395 15-20 minutes, where $\Delta d < 10\%$ was observed.

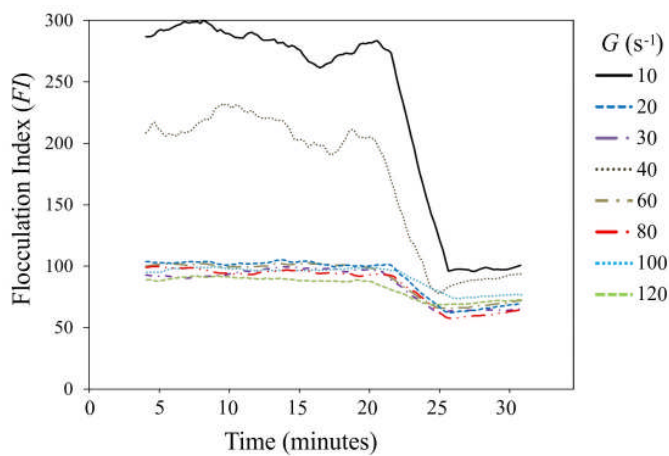
396 3.2 Light scattering

397 Figure 6 shows the temporal evolution of the FI signal (obtained by PDA) in the tests carried
398 out. It is clearly observed that in the flocculation [0-20 minutes] and regrowth [25-40 minutes]
399 phases, the floc size tend towards a stabilized plateau. The sharp drop of FI at 25 minutes was
400 the point where the induced breakage occurred. The difference in the signal scale between the
401 two study waters is caused by the different light scattering properties, *e.g.* floc density and
402 scattering cross-section, which are also dependent on both particle concentration (in terms of
403 volume, mostly) and type (Gregory, 2009). This difference has important implications for the
404 monitoring of floc size by light scattering methods as also observed by Yu *et al.* (2015).
405 Similar fluctuation on FI values were observed by Gregory (2009), while studying optical
406 properties of flocs using PDA for different waters. The author concluded that scattering
407 cross-section is expected to be different when different concentration of impurities, as clay,
408 are within flocs and so FI signals vary. However, the results obtained by Gregory (2009) have
409 shown that curves are rather similar in shape, showing the same relative increase in FI during
410 floc formation. Therefore, although scattering properties can limit direct comparisons of FI
411 values among different waters, it is not expected to affect the strength factor (SF) given by
412 Equation 4, once it is determined as a ratio for the same water, *i.e.* subjected to the same
413 scattering properties.

414



415 a) b)



416

417 Figure 6. Time evolution of FI for different velocity gradients, G before and after induced
 418 breakage using 800 s^{-1} at time 25 minutes. (a) water type 1 for Al-Humic acid and (b) water
 419 type 2 for Al-Kaolin.

420 3.3 Combined analyses of image and photometric dispersion methods

421 Both analyses of image and photometric dispersion methods permitted to compare and
 422 correlate data obtained from two different techniques *i.e.* intrusive and non-intrusive methods.
 423 Tables 1 and 2 present a comparison between the stable size and the floc strength for eight
 424 different velocity gradients (G). The floc strength indicators presented are local stress (σ) and
 425 the force factor (SF).

426 It is observed that, for each of the studied waters, SF , σ and d were strongly correlated with
 427 the parameter G , resulting in Pearson correlation coefficient of 0.95, 0.99 and -0.89 for Al-
 428 Humic and of 0.90, 0.99 and -0.80 for Al-Kaolin, respectively. Results found here corroborate
 429 well with Li *et al.* (2007), who found that flocs formed at higher shear intensities have a small
 430 size and are more resistant to breakage than those formed from lower ones. Floc resistance is

431 determined by both hydraulic shear rates and the strength of flocs bonds, which withstand
432 shear forces during floc formation (Jarvis *et al.*, 2005; Gregory, 2009). During floc formation
433 in high shear rates, the weak bonds might be broken, promoting a kind of selection, which
434 results in floc fragments with strong bonds. Therefore, with the higher shear rates, only the
435 strongest bonds, which are more likely to resist to the abrupt G variations, are maintained (Li
436 *et al.*, 2007). This fact was shown by the increase in SF value from 29.7% for G of 20 s^{-1} to
437 78.6% for G of 120 s^{-1} in water type 1 and 33.3% for G of 20 s^{-1} to 85.2% for G of 120 s^{-1} in
438 water type 2.

439 Results in Tables 1 and 2 also suggested that the effect of G on SF might be more relevant for
440 G from 20 to 40 s^{-1} , and that d values can also decrease dramatically with the increase of G ,
441 indicating there might be a limit above which floc strength is slightly affected by shear rate,
442 but it can strongly affect floc formation.

443 Results obtained from the two other strength indices used here seem to agree with the strength
444 coefficient (γ) analysis. The values of σ were nearly the same for water types 1 and 2, ranging
445 from 0.08 to 0.47 and from 0.07 to 0.44, respectively, with Pearson correlation coefficient (r)
446 between waters near to 1 ($r = 0.97$). These results are in agreement with previous work done
447 by Bache *et al.* (1999) who found Al-Humic flocs strength in the range of 0.08 to 0.42 N/m^2 ,
448 and close to the study by Li *et al.* (2007), who found Al-Kaolin flocs strength in the range of
449 0.01 to 0.24 N/m^2 . Moreover, ANOVA test for σ variation with G indicates that floc strength
450 is not different between Al-Humic and Al-Kaolin for 0.05 of significance (p-value over 0.05),
451 but it depends on G and d only.

452 Regarding the strength factor (SF), results also have shown slight differences between
453 aggregates formed from Al-Humic and Al-Kaolin. Again, the ANOVA test for SF with G
454 indicates that floc strength is not different between Al-Humic and Al-Kaolin for 0.05 of
455 significance, but it depends on G and d only.

456 Despite the fact that the intrinsic characteristics of flocs formed from Al-Kaolin and Al-
457 Humic, namely, the scattering cross-section, altered FI measurements it seems that it did not
458 affect floc strength measurements by SF , as it is in agreement with the other two strength
459 indicators. Therefore, it is not expected that optical proprieties affect physical proprieties
460 measurements, such as resistance, and so the FI signal has been used by many researchers as

461 an aggregation indicator and as well as an indirect measurement of floc strength, *e.g.* Li *et al.*
 462 (2007), Yu *et al.* (2010b and 2011), Su *et al.* (2017).

463

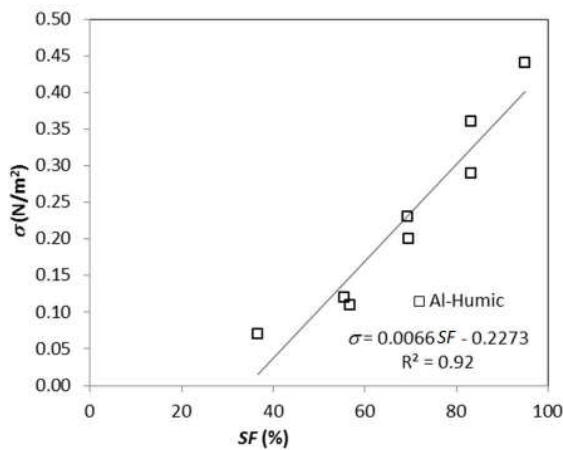
G (s^{-1})	SF (%)	σ N/m ²	d μm
20	36.73	0.07	337
30	56.82	0.11	287
40	55.56	0.12	200
50	69.70	0.20	245
60	69.34	0.23	217
80	83.33	0.29	173
100	83.33	0.36	157
120	95.00	0.44	146

G (s^{-1})	SF (%)	σ N/m ²	d μm
20	33.33	0.08	407
30	35.56	0.09	236
40	61.82	0.17	298
50	65.42	0.16	197
60	58.00	0.24	228
80	62.00	0.36	217
100	78.00	0.39	167
120	85.23	0.47	154

Table 1. Shear rates (G), strength indexes (SF and σ) and stable size (d) for water type 1 (Al-Humic acid) during flocculation.

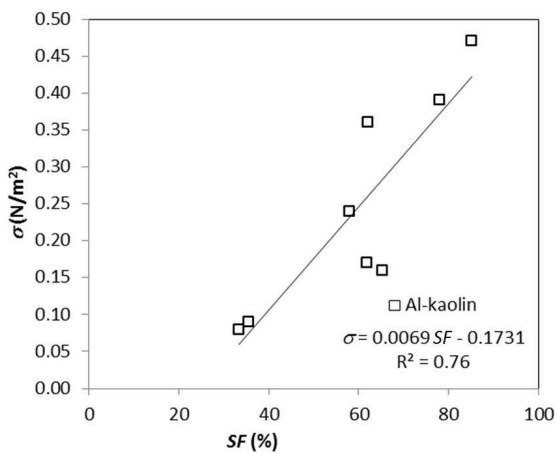
Table 2. Shear rates (G), strength indexes (SF and σ) and stable size (d) for water type 2 (Al-Kaolin) during flocculation.

464 Figure 7 shows the relationship of the strength factor (SF), obtained from PDA, with the
 465 parameter σ , which was calculated from image analysis data. It is observed that for both water
 466 types, relatively high regression coefficients are obtained between SF and σ (R^2 of 0.92 and
 467 0.76 for Al-Humic and Al-Kaolin, respectively) and a similar slope (close to 0.0070) is found
 468 for σ/SF . It is apparent that the values of both mentioned parameters enhance with increase in
 469 G , which are in agreement with results presented by Li *et al.* (2007) and Jarvis *et al.* (2005).
 470 Further, Pearson correlation coefficient between SF and σ resulted in 0.96 and in 0.87 for Al-
 471 Humic and Al-Kaolin, respectively. These strong correlations have confirmed that the
 472 macroscopic approach represented by SF is consistent with the theoretical method for
 473 different types of water, despite of the different methods used and the variations of FI signals.



474 a)

b)



475

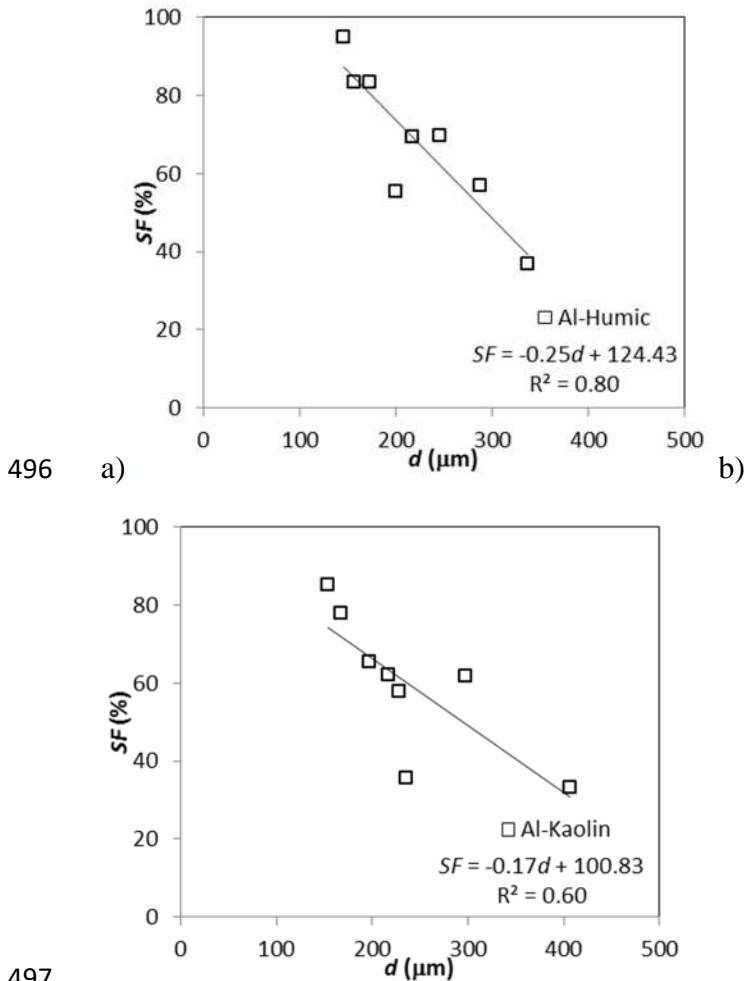
476 Figure 7. Relationship between SF and σ for (a) water type 1 for Al-Humic acid and (b) water
 477 type 2 for Al-Kaolin.

478 Figure 8 shows the relationship between SF and d , *i.e.* the specific relationship between the
 479 strength force indicator obtained from PDA and values of average floc length, monitored by
 480 image analysis. The strength factor (SF) behaved nearly the same as d varied for Al-Humic
 481 and Al-Kaolin flocs, with smaller flocs resulting in higher resistant to G variations. These
 482 results are in agreement with the other strength indicator reported here (Table 1 and 2).

483 Moreover, despite of the differences between the two methods (PDA and image analysis),
 484 results indicate that the parameter d , derived from the non-intrusive image analysis, and SF ,
 485 obtained from the *PDA* signal, behaved in similar way, with R^2 values near to 0.80 for Al-
 486 Humic and 0.60 for Al-Kaolin.

487 The lower R^2 value for Al-Kaolin is believed to be attributed to the different scattering area,
 488 as previously discussed. However, this does not explain why SF for Al-Humic and Al-Kaolin
 489 behaved with no significant difference (p -value over 0.05), when exposed to rupture shear rate

490 of 800 s^{-1} . A possible explanation is that flocs formed from sweep coagulation mechanism are
 491 bigger than those formed from charge neutralization and their physical properties are likely
 492 determined by coagulant only, as pointed out by Yu *et al.* (2015). Besides, floc characteristic
 493 size was calculated based on the average of longest length, and so, it is expected that large
 494 flocs are more prone to breakage by fragmentation when exposed to micro-scale dissipating
 495 eddies, thus resulting in similar strength for Al-Humic and Al-Kaolin aggregates.



497
 498 Figure 8. Relationship between SF and d : (a) water type 1 – Al-Humic and (b) water type 2 –
 499 Al-Kaolin.

500 **4. Conclusions**

501 Floc size and strength play an important role in separation processes used in water and
 502 wastewater treatment, and the influence of different primary particles on the floc strength is
 503 still poorly understood. The evidence that aggregates resistance is invariable with particles
 504 when sweep coagulation is applied needs to be further investigated. Here, two aggregates
 505 formed by Al-Humic and Al-Kaolin during flocculation were investigated using two
 506 techniques, namely intrusive photometric dispersion analyser and non-intrusive image system.

507 Both techniques were applied to determine three floc strength indexes: the strength factors
508 (SF), the local stress (σ) and floc strength coefficient (γ). The main conclusions of this work
509 are:

510

- 511 1. For Al-Humic and Al-Kaolin flocs, the strength factors (SF) and the local stress
512 (σ) have a positive variation in response to the increase of G because the high shear
513 forces select the strongest bonds within the aggregates. This means that higher G
514 produces more resistant aggregates, however the size dependence for an individual
515 separation process efficiency must be considered.
- 516 2. The comparison between the aggregates strength for Al-Humic acid and Al-Kaolin
517 using floc strength coefficient (γ) indicates that both aggregates have nearly the same
518 resistance, possible due to the precipitate hydroxide of alum mostly influencing floc
519 size and strength. This finding reinforces the perspective that particles within a floc
520 may have slight, or even no influence, on the floc strength when sweep coagulation is
521 applied.
- 522 3. The intrusive photometric dispersion analyser and non-intrusive image-based system
523 used in this study produced well correlated parameters, with a similar behaviour.
524 However, the non-intrusive image method proved to be more reliable, as images are
525 not influenced by the optical characteristics of the flocs.

526 **Acknowledgements**

527 Rodrigo B. Moruzzi is grateful to São Paulo Research Foundation (*Fundação de Amparo à*
528 *Pesquisa do Estado de São Paulo—FAPESP*) Proc. 2017/19195-7 for financial support.

529 **References**

- 530 1. Bache, D.H. Floc rupture and turbulence: a framework for analysis. *Chem. Eng. Sci.*
531 59, 2521–2534. (2004). doi: <http://dx.doi.org/10.1016%2Fj.ces.2004.01.055>
- 532 2. Bache, D.H., Al-Ani, S.H. Development of a system for evaluating floc strength.
533 *Water Sci. Technol.* 21, 529–537. (1989). doi: <https://doi.org/10.2166/wst.1989.0255>
- 534 3. Bache, D.H., Johnson, C., McGilligan, J.F., Rasool, E. A conceptual view of floc
535 structure in the sweep floc domain. *Water Sci. Technol.* 36 (4), 49–56. (1997). doi:
536 [https://doi.org/10.1016/S0273-1223\(97\)00418-6](https://doi.org/10.1016/S0273-1223(97)00418-6)

537 4. Bache, D.H., Rasool, E., Moffatt, D., McGilligan, F.J. On the strength and character of
538 alumino-humic floccs. *Water Sci. Technol.* 40 (9), 81–88. (1999). doi:
539 [https://doi.org/10.1016/S0273-1223\(99\)00643-5](https://doi.org/10.1016/S0273-1223(99)00643-5)

540 5. Bache, D.H., Rasool, E.R. Characteristics of alumina humic floccs in relation to DAF
541 performance. *Water Sci. Technol.* 43 (8), 203–208. (2001). doi:
542 <https://doi.org/10.2166/wst.2001.0495>

543 6. Biggs, C.A., Lant, P.A. Activated sludge flocculation: on-line determination of floc
544 size and the effect of shear. *Water Res.* 34, 2542–2550. (2000).

545 7. Chakraborti, R. K.; Gardner, K. H.; Atkinson, J. F.; Van Benschoten, J. E. Changes in
546 fractal dimension during aggregation. *Water Research.* v.37. p. 873–883. (2003).

547 8. Francois, R.J. Strength of aluminium hydroxide floccs. *Water Res.* 21, 1023–1030
548 (1987). doi: [https://doi.org/10.1016/0043-1354\(87\)90023-6](https://doi.org/10.1016/0043-1354(87)90023-6)

549 9. Gregory and D.W. Nelson, A new optical method for flocculation monitoring. In
550 *Solid-Liquid Separation* (J. Gregory, Ed.) Ellis Horwood, Chichester, pp 172-182.
551 (1984).

552 10. Gregory, J. Monitoring particle aggregation process. *Advances in Colloids and*
553 *Interfaces* v.147-148, 109-123. (2009). doi: <https://doi.org/10.1016/j.cis.2008.09.003>

554 11. Gregory, J. Optical monitoring of particle aggregates. *J. Environ. Sci.* 21, 2e7. (2009).
555 doi: [https://doi.org/10.1016/S1001-0742\(09\)60002-4](https://doi.org/10.1016/S1001-0742(09)60002-4)

556 12. Gregory, J., Monitoring floc formation and breakage. In: *Proceedings of the Nano and*
557 *Micro Particles in Water and Wastewater Treatment Conference.* International Water
558 Association, Zurich September (2003)

559 13. Gregory, J., Nelson, D.W. Monitoring of aggregates in flowing suspension. *Colloids*
560 *Surf.* 18, 175–188, (1986).

561 14. Jarvis P., Jefferson B., Gregory, J. and Parsons, S. A. A review of floc strength and
562 breakage. *Water Res.* 39, 3121-3137. (2005). doi:
563 <http://dx.doi.org/10.1016/j.watres.2005.05.022>

564 15. Li, T. Zhu, Z., Wang, D., Yao, C. and Tang, H. The strength and fractal dimension
565 characteristics of alum–kaolin floccs. *International Journal Of Mineral Processing,*
566 Beijing, Pr China, v. 82, n. 1, 23-29. (2007). doi: [https://doi.org/10.1016/S0273-](https://doi.org/10.1016/S0273-1223(99)00643-5)
567 [1223\(99\)00643-5](https://doi.org/10.1016/S0273-1223(99)00643-5)

568 16. Leentvaar, J., Rebhun, M. Strength of ferric hydroxide floccs. *Water Res.* 17, 895–902.
569 (1983).

- 570 17. Mikkelsen, L.H., Keiding, K. The shear sensitivity of activated sludge: an evaluation
571 of the possibility for a standardised floc strength test. *Water Res.* 36, 2931–2940.
572 (2002). doi: [https://doi.org/10.1016/S0043-1354\(01\)00518-8](https://doi.org/10.1016/S0043-1354(01)00518-8)
- 573 18. Mühle, K. Floc stability in laminar and turbulent flow. In: Dobias, B. (Ed.),
574 Coagulation and Flocculation. Dekker, New York, pp. 355–390. (1993).
- 575 19. Oliveira, A.L. de, Moreno, P., Silva, P.A.G. da, Julio, M.D. and Moruzzi, R.B. Effects
576 of the fractal structure and size distribution of flocs on the removal of particulate
577 matter. *Desalination and Water Treatment.*, Vol. 57 (36). 1–12. (2015). doi:
578 <https://doi.org/10.1080/19443994.2015.1081833>
- 579 20. Parker, D.S., Kaufman, W.J., Jenkins, D. Floc breakup in turbulent flocculation
580 processes. *J. Sanit. Eng. Div.: Proc. Am. Soc. Civ. Eng. SA1*, 79–99. (1972). doi:
581 <https://pubs.acs.org/doi/abs/10.1021/la980763o>
- 582 21. Moruzzi, R. B., Silva, P. A. G. Reversibility of Al-Kaolin and Al-Humic aggregates
583 monitored by stable diameter and size distribution. *Brazilian Journal of Chemical*
584 *Engineering.*, Vol. 35 (3). 1029–1038. (2018). doi: [dx.doi.org/10.1590/0104-](dx.doi.org/10.1590/0104-6632.20180353s20170098)
585 [6632.20180353s20170098](dx.doi.org/10.1590/0104-6632.20180353s20170098)
- 586 22. Zhaoyang Su, Xing Li, Yanling Yang. Regrowth ability and coagulation behavior by
587 second dose: Breakage during the initial flocculation phase. *Colloids and Surfaces A*
588 527, 109–114. (2017). doi: <http://dx.doi.org/10.1016/j.colsurfa.2017.05.034>
- 589 23. Wang, Y., Gao, B., Xu, X., Xua, W., Xub, G. Characterization of floc size, strength
590 and structure in various aluminum coagulants treatment. *Journal of Colloid and*
591 *Interface Science* v332, 354–359. (2009). doi:
592 <https://doi.org/10.1016/j.jcis.2009.01.002>
- 593 24. Watanabe, Y., Flocculation and me. *Water Research.* (2017). doi:
594 <https://doi.org/10.1016/j.watres.2016.12.035>
- 595 25. Yu, W., Gregory, J. and Campos, L. The effect of additional coagulant on the re-
596 growth of alum–kaolin flocs. *Separation and Purification Technology* v74, 305–309.
597 (2010a). doi: <https://doi.org/10.1016/j.seppur.2010.06.020>
- 598 26. Younker, J. M., Walsh, M. E. Effect of adsorbent addition on floc formation and
599 clarification. *Water Research* 98. (2016). doi:
600 <https://doi.org/10.1016/j.watres.2016.03.044>

- 601 27. Yu, W., Gregory, J. and Campos, L., Breakage and Regrowth of al Humic Floccs –
602 Effect of additional Coagulant Dosage. *Environ. Sci. Technol*, no. 44. (2010b). doi:
603 <http://dx.doi.org/10.1021/es1007627>
- 604 28. Yu, W., Gregory, J., Campos, L., Breakage and re-growth of floccs: Effect of additional
605 doses of coagulant species. *Water Research*, 45. (2011). doi:
606 <https://doi.org/10.1016/j.watres.2011.10.016>
- 607 29. Yu, W., Gregory, J., Campos, L., Graham, N. Dependence of flocc properties on
608 coagulant type, dosing mode and nature of particles. *Water Research* 68, p 119-126.
609 (2015). doi: <https://doi.org/10.1016/j.watres.2014.09.045>
- 610 30. Yu, W., Hu, C., Liu, H., Qu, J. Effect of dosage strategy on Al-humic floccs growth and
611 re-growth. *Colloids and Surfaces A: Physicochem. Eng. Aspects*, 404, 106–111.
612 (2012). doi: <https://doi.org/10.1016/j.colsurfa.2012.04.033>
- 613 31. Yukselen, M. A. and Gregory, J. The reversibility of floccs breakage. *International*
614 *Journal of Mineral Processing*, v. 73, no. 2-4, p. 251-259. (2004). doi:
615 [https://doi.org/10.1016/S0301-7516\(03\)00077-2](https://doi.org/10.1016/S0301-7516(03)00077-2)
- 616 32. Yukselen, M.A. and Gregory, J. Breakage and reformation of alum floccs. *Environ.*
617 *Eng. Sci.* no. 19, p. 229–236. (2002). doi:
618 <https://doi.org/10.1089/109287502760271544>
- 619 33. Zhong, R., Zhang, X., Xiao F., Li, X., Cai Z., Effects of humic acid on physical and
620 hydrodynamic properties of kaolin floccs by particle image velocimetry. *Water*
621 *Research* 45. (2011). doi: <https://doi.org/10.1016/j.watres.2011.05.006>